

## PHYSIOLOGY

## Reduced MC4R signaling alters nociceptive thresholds associated with red hair

Kathleen C. Robinson<sup>1\*</sup>, Lajos V. Kemény<sup>1\*</sup>, Gillian L. Fell<sup>1†</sup>, Andrea L. Hermann<sup>1,2</sup>, Jennifer Allouche<sup>1</sup>, Weihua Ding<sup>3</sup>, Ajay Yekkirala<sup>4</sup>, Jennifer J. Hsiao<sup>1</sup>, Mack Y. Su<sup>1</sup>, Nicholas Theodosakis<sup>1</sup>, Gabor Kozak<sup>5,6</sup>, Yuichi Takeuchi<sup>5,7,8,9</sup>, Shiqian Shen<sup>3</sup>, Antal Berenyi<sup>5,8,10,11</sup>, Jianren Mao<sup>3</sup>, Clifford J. Woolf<sup>4</sup>, David E. Fisher<sup>1‡</sup>

Humans and mice with natural red hair have elevated basal pain thresholds and an increased sensitivity to opioid analgesics. We investigated the mechanisms responsible for higher nociceptive thresholds in red-haired mice resulting from a loss of melanocortin 1 receptor (MC1R) function and found that the increased thresholds are melanocyte dependent but melanin independent. MC1R loss of function decreases melanocytic proopiomelanocortin transcription and systemic melanocyte-stimulating hormone (MSH) levels in the plasma of red-haired (*Mc1r<sup>el/e</sup>*) mice. Decreased peripheral  $\alpha$ -MSH derepresses the central opioid tone mediated by the opioid receptor OPRM1, resulting in increased nociceptive thresholds. We identified MC4R as the MSH-responsive receptor that opposes OPRM1 signaling and the periaqueductal gray area in the brainstem as a central area of opioid/melanocortin antagonism. This work highlights the physiologic role of melanocytic MC1R and circulating melanocortins in the regulation of nociception and provides a mechanistic framework for altered opioid signaling and pain sensitivity in red-haired individuals.

## INTRODUCTION

Humans and mice with red hair exhibit altered pain thresholds, increased nonopioid analgesic requirements, and enhanced responses to opioid analgesics (1–6). Red hair in both species is caused by loss-of-function variant alleles of the melanocortin 1 receptor (MC1R), a  $G\alpha_s$ -coupled receptor expressed on melanocytes, the pigment-producing cells of the skin (7). MC1R mutant red-haired mice are less sensitive to noxious thermal, mechanical, and chemical stimuli (4). However, the mechanism of this altered nociception has not been determined, prompting us to examine the mechanistic connection between MC1R and the modulation of nociception.

MC1R function is suppressed in the *Mc1r<sup>el/e</sup>* mouse strain because of a frameshift mutation resulting in a premature stop codon. This strain (referred to herein as red-haired mice) has yellow/red hair and recapitulates features of red-haired humans including synthesis of red/blond pheomelanin pigment, inability to tan following UV

exposure, and increased ultraviolet (UV)-associated skin cancer risk (8, 9).

## RESULTS

To initially assess nociceptive thresholds in *Mc1r<sup>el/e</sup>* mice in a blinded fashion and to test the role of pigment (versus red-haired genetic background) in nociception, we crossed *Mc1r<sup>el/e</sup>* mice with an albino strain containing a loss-of-function mutation in the tyrosinase gene (*Tyr<sup>c/c</sup>*). In these mice, melanocyte numbers are not altered, but they are unpigmented (fig. S1). Double mutant *Mc1r<sup>el/e</sup>;Tyr<sup>c/c</sup>* mice are visually indistinguishable from *Tyr<sup>c/c</sup>* mice, as both have white hair. After “unblinding” the measurements, mice homozygous for the red hair allele (*Mc1r<sup>el/e</sup>*) exhibited significantly higher nociceptive thresholds for both pressure and temperature relative to *Mc1r<sup>E/E</sup>* wild-type (WT) mice in the albino genetic background (*Tyr<sup>c/c</sup>*) (Fig. 1, A and B). Similarly, increased nociceptive thresholds were observed for *Mc1r<sup>el/e</sup>* mice compared with *Mc1r<sup>E/E</sup>* mice in the non-albino *Tyr<sup>+/+</sup>* C57BL/6J background (Fig. 1, C and D), in agreement with previous observations (4). This finding suggests a pigment-independent role of MC1R in the regulation of nociception.

To determine whether the increased nociceptive thresholds in red-haired mice are caused by MC1R loss of function within melanocytes or in other cell types, we compared three genetically matched (C57BL/6J) mouse models that differ in melanocyte numbers (summarized in table S1). Mice with increased numbers of epidermal melanocytes (K14-SCF) exhibited significantly lower nociceptive thresholds (Fig. 1, E and F), while mice lacking melanocytes (*Mitf<sup>mi-wh/mi-wh</sup>*) displayed higher nociceptive thresholds compared with WT mice (Fig. 1, G and H). These findings suggest that the number of epidermal melanocytes (independent of MC1R function) can modulate nociceptive thresholds. Next, we crossed red-haired mice with *Mitf<sup>mi-wh/mi-wh</sup>* mice. Because *Mitf<sup>mi-wh/mi-wh</sup>* mice completely lack melanocytes, this comparison between “red-haired” *Mc1r<sup>el/e</sup>;Mitf<sup>mi-wh/mi-wh</sup>* and “black-haired” *Mc1r<sup>E/E</sup>;Mitf<sup>mi-wh/mi-wh</sup>* groups tests potential MC1R

<sup>1</sup>Cutaneous Biology Research Center, Department of Dermatology and MGH Cancer Center, Massachusetts General Hospital, Harvard Medical School, Boston, MA 02129, USA. <sup>2</sup>Doctoral School of Clinical Medicine, University of Szeged, Szeged 6720, Hungary. <sup>3</sup>MGH Center for Translational Pain Research, Department of Anesthesia, Critical Care and Pain Medicine, Massachusetts General Hospital, Harvard Medical School, Boston, MA 02129, USA. <sup>4</sup>FM Kirby Neurobiology Center, Boston Children’s Hospital, and Department of Neurobiology, Harvard Medical School, Boston, MA 02115, USA. <sup>5</sup>MTA-SZTE ‘Momentum’ Oscillatory Neuronal Networks Research Group, Department of Physiology, Interdisciplinary Excellence Centre, University of Szeged, Szeged H-6720, Hungary. <sup>6</sup>University Neurology Hospital and Hertie Institute for Clinical Brain Research, Tübingen, Germany. <sup>7</sup>Department of Neuropharmacology, Graduate School of Pharmaceutical Sciences, Nagoya City University, Nagoya 467-8603, Japan. <sup>8</sup>Neurocybernetics Excellence Center, University of Szeged, 10 Dom sqr, Szeged 6720, Hungary. <sup>9</sup>Department of Physiology, Osaka City University Graduate School of Medicine, 1-4-3, Asahimachi, Abeno-ku, Osaka 545-8585, Japan. <sup>10</sup>Neuroscience Institute, New York University, New York City, NY 10016, USA. <sup>11</sup>HCEMM-USZ Magnetotherapeutics Research Group, University of Szeged, 10 Dom sqr, Szeged 6720, Hungary.

\*These authors contributed equally to this work.

†Present address: Department of Surgery, Brigham and Women’s Hospital, 75 Francis Street, Boston, MA 02115, USA.

‡Corresponding author. Email: dfisher3@mgh.harvard.edu

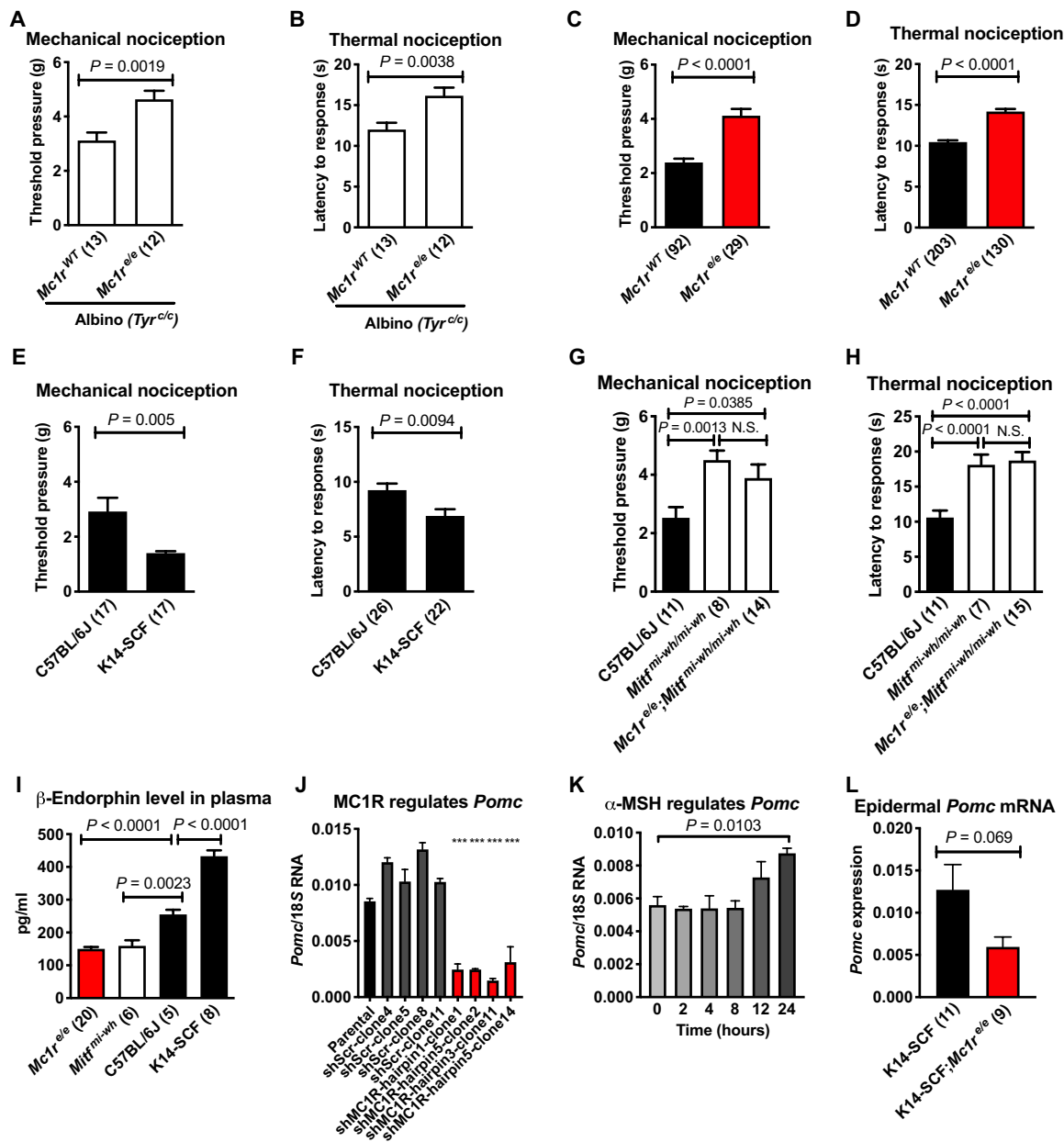


**Fig. 1. Nociceptive thresholds and POMC production are affected by melanocyte status and MC1R signaling.** Loss of function of MC1R increases mechanical and thermal nociceptive thresholds in C57BL/6J *Tyr<sup>cl/c</sup>* albino mice (A and B) and in non-albino C57BL/6J mice (C and D). Nociceptive thresholds are decreased in K14-SCF strain compared with C57BL/6J mice measured by both von Frey assay (E) and hot plate assay (F). *Mc1r*<sup>e/e</sup>; *Mitf*<sup>mi-wh/mi-wh</sup> double mutants had increased thresholds compared with C57BL/6J, but similar to *Mitf*<sup>mi-wh/mi-wh</sup>, by von Frey (G) and hot plate assays (H). (I) Levels of β-endorphin in blood plasma were assayed by radioimmunoassay, suggesting MC1R-dependent melanocytic regulation of POMC. (J) sh*Mc1r* in the mouse melanocytic Melan-C cell line decreases *Pomc* mRNA expression. \*\*\*\* $P < 0.001$  compared with all of the shControl clones and the parental line. (K) The MC1R ligand α-MSH (2 μM) increases *Pomc* production in Melan-C cells. (L) *Pomc* expression is decreased in the epidermal skin of red K14-SCF;*Mc1r*<sup>e/e</sup> mice compared with black K14-SCF;*Mc1r*<sup>WT</sup> mice. Graphs show means ± SEM; numbers in parentheses = *n* per group. Data shown in (C) and (D) represent compilations of baseline thresholds from all black and red-haired male mice in the C57BL/6J background used in the study. Results in (E) and (F) are a compilation of two and three independent experiments, respectively. Each group in (J) and (K) consists of three biological replicates. N.S., not significant.

function in nonmelanocytic cells. As shown in Fig. 1 (G and H), genetic absence of melanocytes ablated the ability of MC1R to influence nociceptive thresholds, suggesting that altered thresholds are dependent on MC1R function in melanocytes rather than in other cell types.

One potential modulator of the elevated nociceptive threshold in red-haired mice is β-endorphin, a posttranslational cleavage product of proopiomelanocortin (POMC), which is expressed in melanocytes (10–12). POMC is induced by adenosine 3',5'-monophosphate (cAMP) in other cell types (13, 14); thus, low cAMP levels in *Mc1r*

mutant melanocytes may affect POMC expression. Red-haired ( $Mcl1^{e/e}$ ) mice had significantly lower plasma levels of  $\beta$ -endorphin than genetically matched black (C57BL/6J WT) mice (Fig. 1I). However, this difference did not suggest that changes in  $\beta$ -endorphin mediate altered nociceptive thresholds because the direction of change is opposite from the phenotypic change, since opioid signaling promotes rather than diminishes analgesia. Moreover, plasma levels of  $\beta$ -endorphin were also inversely associated with nociceptive thresholds in K14-SCF mice (higher melanocyte numbers and lower nociceptive thresholds) and  $Mitf^{mi-wh/mi-wh}$  mice (absent melanocytes and higher nociceptive thresholds). Collectively, these data demonstrated a consistent pattern in which melanocyte numbers (K14-SCF,  $Mitf^{mi-wh/mi-wh}$ ) and function ( $Mcl1^{E/E}$ ,  $Mcl1^{e/e}$ ) were inversely correlated with nociceptive thresholds despite being directly related to circulating  $\beta$ -endorphin levels.

To test for a direct role of melanocytes in modulating POMC expression downstream of MC1R, we knocked down  $Mcl1$  mRNA (Fig. 1J) or stimulated MC1R with  $\alpha$ -melanocyte-stimulating hormone ( $\alpha$ -MSH) (Fig. 1K) in the mouse melanocyte line Melan-C (15) and observed decreased and increased *Pomc* mRNA production, respectively. Furthermore, isolated epidermal RNA from black (K14-SCF; $Mcl1^{E/E}$ ) and red-haired (K14-SCF; $Mcl1^{e/e}$ ) mice revealed reduced *Pomc* expression in epidermal skin of mice harboring loss of function in MC1R (Fig. 1L), similar to the lower plasma levels of circulating  $\beta$ -endorphin in the red-haired background (Fig. 1I, top). *Pomc* expression did not show statistically significant reduction in the adrenal gland and in the pituitary gland of  $Mcl1^{e/e}$  mice (fig. S2), suggesting that the plasma level alterations of POMC in this genetic background are mainly due to the decrease in melanocytic *Pomc* production caused by loss of *Mcl1* function.

To determine whether the elevated nociceptive thresholds were a result of compensation for or adaptation to the lower  $\beta$ -endorphin levels, we used two genetic models: mice carrying homozygous POMC mutation that expresses all melanocortin peptides but lacks the terminal  $\beta$ -endorphin sequence (“ $\beta$ -endorphin knockout”) and a strain deficient in the  $\beta$ -endorphin receptor gene,  $\mu$ -opioid receptor (*Oprm1*<sup>-/-</sup>). We observed no measurable effect of  $\beta$ -endorphin knockout on the nociceptive threshold differences in black versus red-haired mice (Fig. 2, A and B), suggesting that  $\beta$ -endorphin expression does not account for the altered nociceptive thresholds, as anticipated because its levels were inversely related to phenotypes. *Oprm1* deletion had no effect on nociceptive thresholds in black mice, in agreement with previous observations (16, 17) and supporting the hypothesis that basal nociceptive thresholds in WT C57BL/6 mice are unaffected by endogenous opioids (18, 19). However, the absence of OPRM1 abolished the elevated thresholds in red-haired mice (Fig. 2, C and D). Similarly, naloxone, a broad opioid receptor antagonist (20), and cyprodime, an antagonist specific for the  $\mu$ -opioid receptor (21), both significantly reduced nociceptive thresholds in red-haired mice to levels in black mice or to even lower levels at high doses (Fig. 2, E and F). A decrease below WT levels was observed only with pharmacologic antagonists and may reflect a difference between acute blockade and chronic absence of signaling.

These findings suggest that the elevated nociceptive thresholds in red-haired mice are mediated by, and dependent on,  $\beta$ -endorphin-independent opioid receptor signaling. We also observed a decrease in nociceptive thresholds when  $Mitf^{mi-wh/mi-wh}$  mice (devoid of melanocytes) were treated with naloxone (Fig. 2G), consistent with a

common endogenous opioid-dependent mechanism for  $Mitf^{mi-wh/mi-wh}$  and red-haired  $Mcl1^{e/e}$  mice.

We reasoned that higher  $\mu$ -opioid receptor signaling in the presence of low plasma levels of  $\beta$ -endorphin could be explained by up-regulation of another endogenous opioid, an adaptation of the  $\mu$ -opioid receptor, or reduction of a pathway that antagonizes opioid signaling. Direct measurements of the circulating opioid ligands dynorphin, enkephalin, and endomorphin revealed no significant differences between red-haired and black mice (Fig. 3, A to C). Given previously published data (2) on differences between red-haired and black mice in their response to pentazocine, a  $\kappa$ -opioid receptor agonist, we chose to further examine the  $\kappa$  receptor agonist dynorphin. We crossed a dynorphin knockout strain with red-haired and black mice but did not observe measurable effects on nociceptive thresholds in red-haired or black genetic backgrounds (Fig. 3, D and E). These data suggest that elevation of an endogenous opioid is unlikely to be responsible for the increased nociceptive threshold in the red hair background.

Pharmacologic manipulation of the melanocortin pathway antagonizes certain effects of morphine (22, 23), leading us to examine plasma levels of MSH (melanocortin agonist), which, like  $\beta$ -endorphin, is also encoded within POMC. We observed that plasma  $\alpha$ -MSH levels varied significantly across mice of different pigmentation phenotypes, paralleling  $\beta$ -endorphin levels as anticipated given their common POMC precursor, with higher  $\alpha$ -MSH levels in mice with more melanocytes or WT MC1R/black pigmentation (Fig. 4A) and lower in mice with fewer melanocytes or red-haired genetic background. Plasma  $\alpha$ -MSH levels therefore vary in a manner that is consistent with and might be responsible for the observed nociceptive phenotypes, unlike  $\beta$ -endorphin that is inversely related. Given that  $\alpha$ -MSH [or its larger parent peptide adrenocorticotrophic hormone (ACTH)] represents the only known melanocortin ligand, whereas  $\beta$ -endorphin is one of multiple endogenous ligands capable of activating  $\mu$ -opioid receptor signaling, a decrease in both  $\alpha$ -MSH and  $\beta$ -endorphin might result in a net increase in opioid signaling sustained by non-POMC-derived opioid ligands. To functionally evaluate whether proportionally low  $\alpha$ -MSH may contribute to the elevated nociceptive thresholds in the red hair background, we first rescued low endogenous  $\alpha$ -MSH levels in red-haired mice pharmacologically. We observed that an  $\alpha$ -MSH peptide mimic, melanotan II, decreased nociceptive thresholds in a dose-dependent fashion in male red-haired  $Mcl1^{e/e}$  mice but not in black  $Mcl1^{E/E}$  mice (Fig. 4B). Second, given the sex-dependent role of *Mcl1* in mediating pharmacologic  $\kappa$ -opioid analgesia (2), we repeated these experiments in female red-haired  $Mcl1^{e/e}$  mice and observed the same patterns as in male red-haired  $Mcl1^{e/e}$  mice (fig. S3, A to D). These results suggest that loss of function in MC1R signaling results in increased nociceptive thresholds because of melanocortin deficiency in a sex-independent (likely  $\kappa$ -opioid-independent) manner. As the MSH mimic-induced rescue phenotype occurred in red-haired mice carrying MC1R deficiency (as a result of an *Mcl1* frameshift mutation), it suggested that an MSH receptor other than MC1R is the likeliest mediator of the altered nociception (and opioid antagonism).

Another melanocortin receptor, MC4R, and its inhibition have been implicated in pharmacologic analgesia and neuropathic pain (23, 24). We initially tested the peptide SHU 9119, which antagonizes MC4R and MC3R while being an agonist for MC1R and MC5R (25). SHU 9119 produced analgesia when injected into male black mice (Fig. 4C), mimicking the effect of the  $Mcl1^{e/e}$  genotype. Similarly,

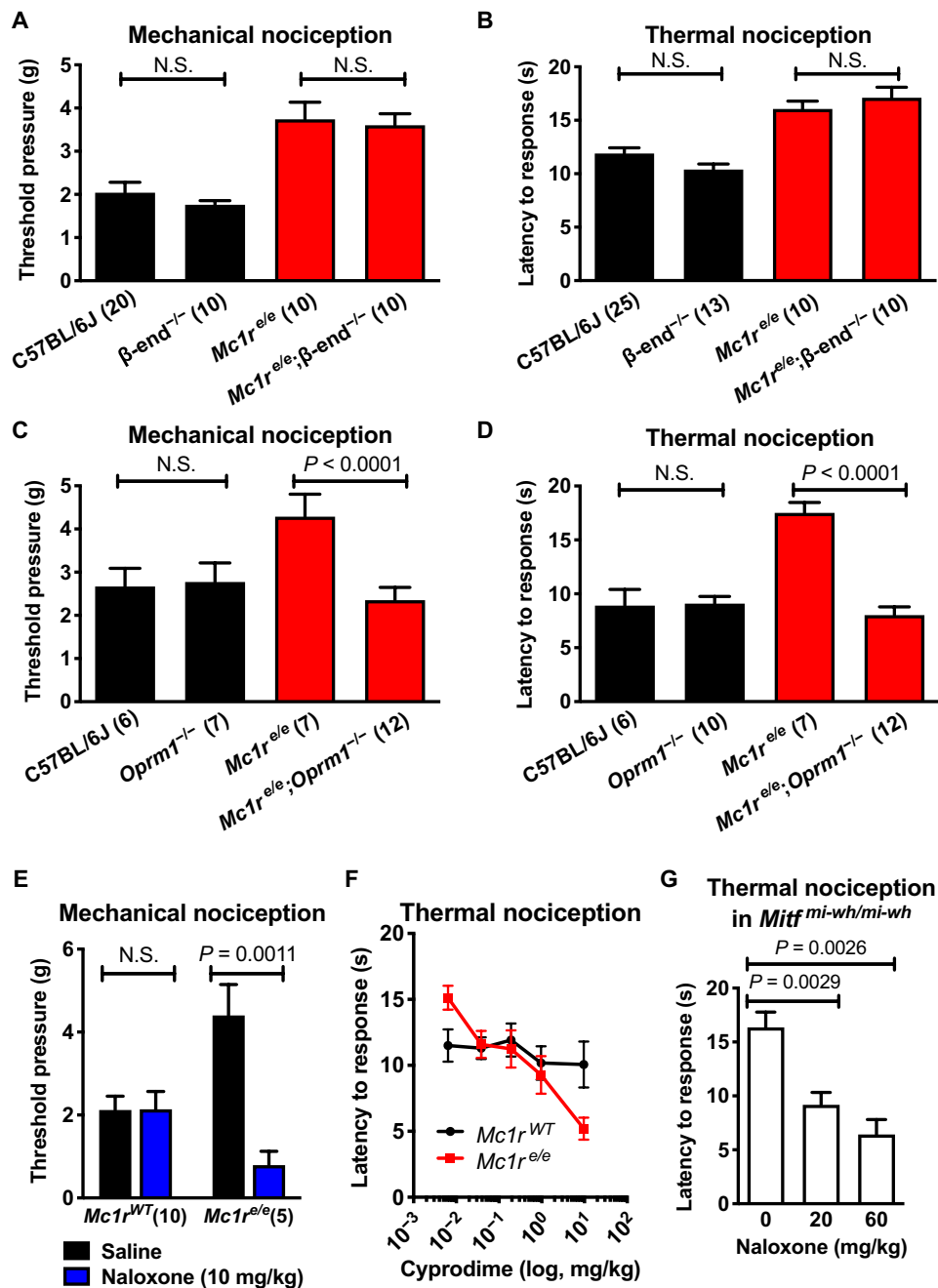


**Fig. 2. Elevated nociceptive thresholds in red-haired mice depend on opioid signaling but not  $\beta$ -endorphin.**  $\beta$ -Endorphin deletion has no effect on mechanical (A) or thermal (B) nociceptive thresholds in either black or red-haired mice (compilations of two independent experiments). Deletion of the  $\mu$ -opioid receptor did not affect nociceptive thresholds in black mice but abolished the increased thresholds in red-haired mice in both mechanical (C) and thermal (D) nociception assays. (E) Naloxone treatment (10 mg/kg, intraperitoneally) abolished the increased nociceptive threshold of red mice. (F) Cyprodime treatment showed a dose-dependent effect on thermal nociception in red-haired, but not black, mice (for *Mc1r*<sup>WT</sup>,  $n = 11$ , except  $n = 10$  for 0.0064 mg/kg; for *Mc1r*<sup>el/e</sup>,  $n = 9$ , except  $n = 7$  for 9.6 mg/kg). (G) Naloxone treatment also decreased nociceptive thresholds in *Mitf*<sup>mi-wh/mi-wh</sup> homozygous mice ( $n = 8$  per group). For (A) to (D), the investigator performing the experiment was blinded to the  $\beta$ -endorphin or OPRM1 status of each mouse. Graphs show means  $\pm$  SEM; numbers in parentheses =  $n$  per group.

in K14-SCF;*Mc1r*<sup>el/e</sup> mice, which have levels of POMC products (fig. S3) and nociceptive thresholds similar to black WT mice (Fig. 4C) but lack MC1R function, injection of SHU 9119 increased nociceptive thresholds. These functional results suggested that the analgesic effects of SHU 9119 are *Mc1r* independent and likely due to ligand

effects on MC4R or MC3R, consistent with the possibility that MC4R or MC3R signaling may balance opioid signaling to modulate nociceptive thresholds.

To explore whether MC4R plays a functional role in regulating nociceptive thresholds, we used *Mc4r* null mice and observed that

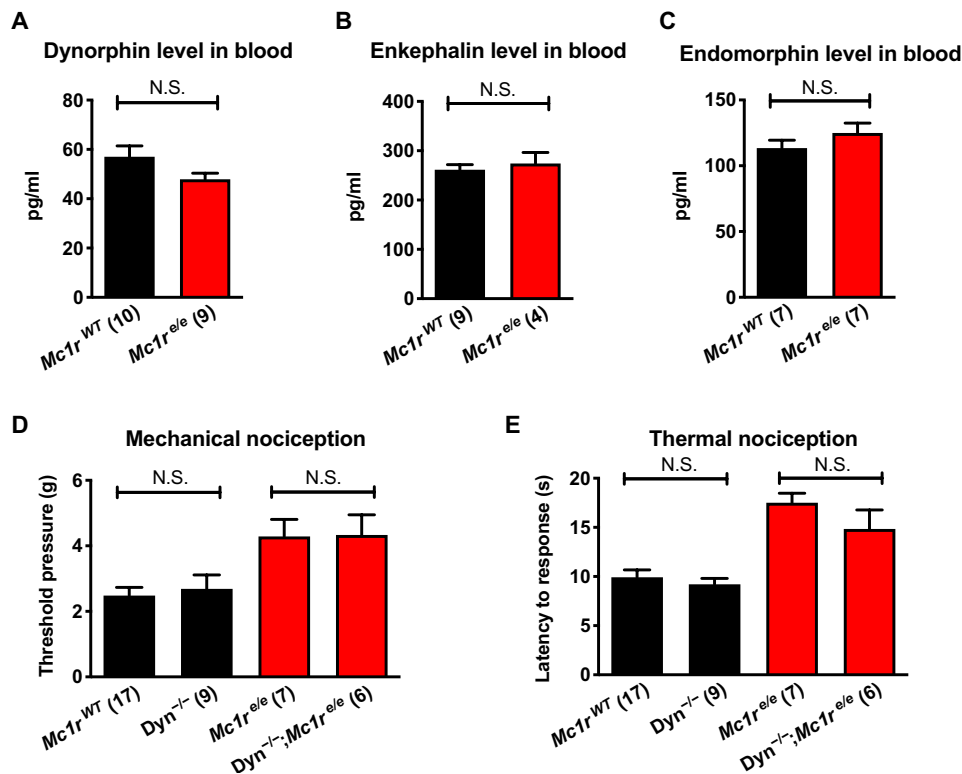


**Fig. 3. Low levels of  $\beta$ -endorphin are not compensated by other endogenous opioids.** (A to C) Plasma levels of dynorphin, enkephalin, and endomorphin are unchanged in red versus black mice. (D and E) Loss of the dynorphin gene (*Dyn<sup>-/-</sup>*) has no effect on nociceptive thresholds in red or black mice. Graphs show means  $\pm$  SEM; numbers in parentheses = *n* per group.

they exhibit elevated nociceptive thresholds (Fig. 4, D and E). The absence of MC4R (on a genetically black *Mc1r<sup>E/B</sup>* background) also resulted in sensitivity to opioid antagonism (Fig. 4F), resembling red-haired *Mc1r<sup>ele</sup>* mice and suggesting that the nociceptive threshold may be determined by a balance between OPRM1 and MC4R signaling. We also repeated this experiment using naloxazine, a specific antagonist for the  $\mu$ -opioid receptor, and found that pharmacologic inhibition of OPRM1 is sufficient to restore nociceptive thresholds in both *Mc4r* null and *Mc1r<sup>ele</sup>* mice (Fig. 4G). Furthermore, melanocortin agonist treatment reduced the elevated nociceptive thresholds in red-haired mice (Fig. 4B) but had no effect on nociception in *Mc4r* null mice (Fig. 4H), suggesting that MC4R is the key melanocortin receptor upon which MSH acts as a ligand for nociceptive threshold reduction.

We hypothesized that if MSH deficiency in *Mc1r<sup>ele</sup>* mice is acting through MC4R, then *Mc1r<sup>ele</sup>; MC4R<sup>-/-</sup>* mice should have similar nociception to *Mc1r<sup>ele</sup>* and MC4R null mice. When we generated *Mc1r<sup>ele</sup>; MC4R<sup>-/-</sup>* mice, we found that *Mc1r<sup>ele</sup>; MC4R<sup>-/-</sup>* mice have similar nociception to *Mc1r<sup>ele</sup>* and MC4R<sup>-/-</sup> mice (Fig. 4I), suggesting that there is a similar underlying mechanism responsible for the elevated nociceptive thresholds in these genetic mouse models.

Next, we asked whether the site of the opioid/melanocortin antagonism modulating nociception is central or peripheral. The nociceptive difference observed between black and red-haired mice was diminished after peripheral (intraperitoneal) administration of naltrexone, an opioid receptor antagonist that is able to cross the blood-brain barrier (BBB) (Fig. 5A). However, peripheral administration of methylated naltrexone, a BBB-impermeable opioid antagonist,

did not diminish the nociceptive differences between black and red-haired mice (Fig. 5B), suggesting minimal peripheral influence. This suggests that the relative increase in opioid signaling in red-haired mice occurs centrally, not peripherally, and highlights the importance of  $\alpha$ -MSH in balancing opioid receptor-mediated regulation of central nociception.

Previous studies have demonstrated a role for cAMP signaling in modulating opioid analgesia (26). We therefore measured the impact of antagonism between melanocortin and opioid signaling on cAMP content in rat primary hypothalamic neurons (RPHNs). We observed that the melanocortin agonist [Nle4,D-Phe7]- $\alpha$ -MSH increased cAMP content, whereas the opioid agonist morphine significantly inhibited melanocortin-induced cAMP elevation (Fig. 5C), consistent with previous observations (27). These data suggest that melanocortin and opioid signaling may antagonize each other in a cell-autonomous manner.

Costaining MC4R-GFP (green fluorescent protein) neurons with OPRM1 in mice has suggested the existence of neurons expressing both receptors in the periaqueductal gray area (PAG) (28). First, we measured the mRNA levels of opioid receptors in the PAG in different genetic backgrounds and found no significant alterations in the opioid receptors in the PAG in *Mc1r<sup>ele</sup>* and *Mc4r<sup>-/-</sup>* mice (fig. S5). We next investigated the potential role of the PAG in modulating nociception and found that local antagonism of opioid receptors by naloxone, by the  $\mu$ -opioid receptor-specific naloxazine (29), or agonism of melanocortin receptors (independently of *Mc1r*) in PAG-cannulated *Mc1r<sup>ele</sup>* mice significantly decreases nociceptive thresholds (Fig. 5D). To further investigate the localization of MC4R



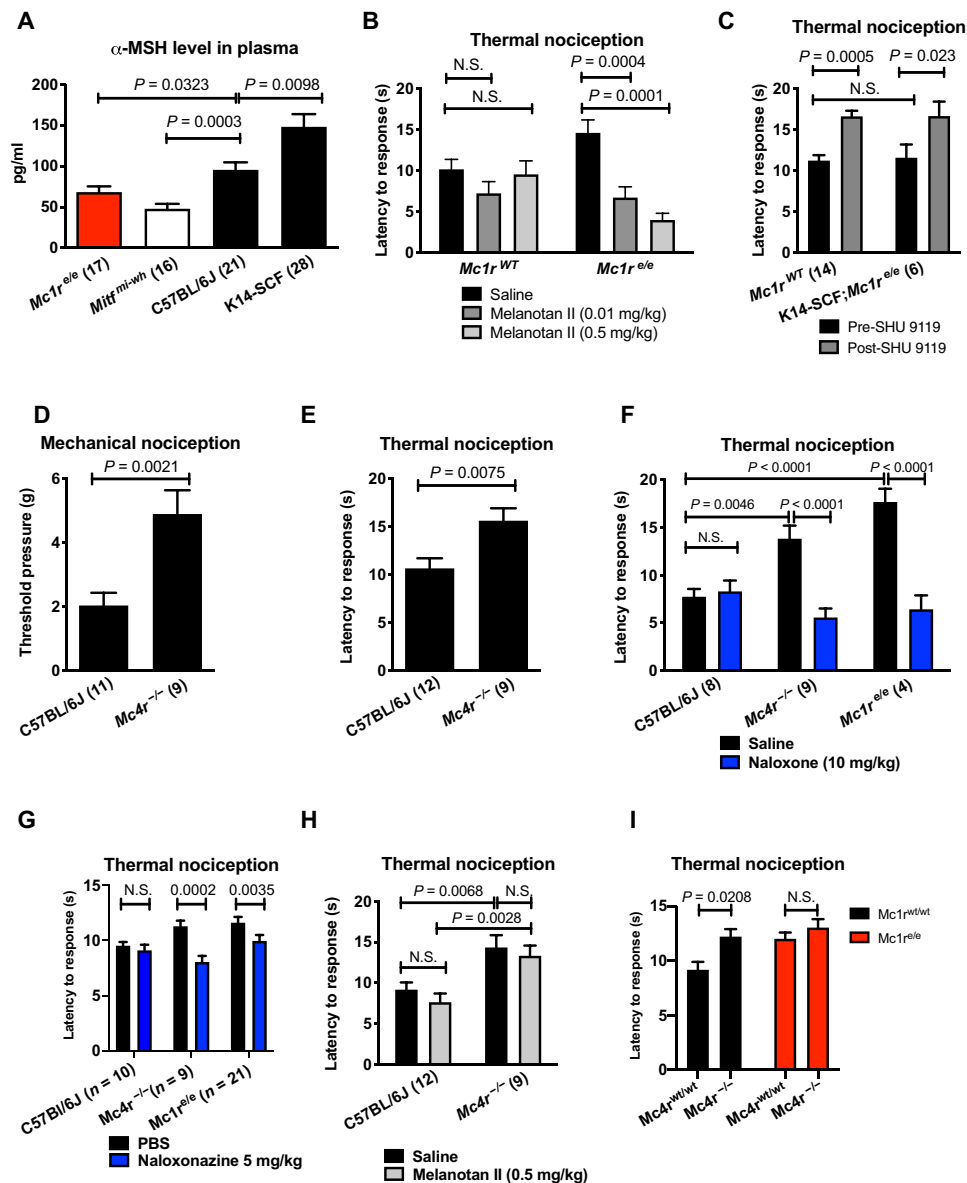


**Fig. 4. MC4R signaling regulates nociception.**  $\alpha$ -MSH in blood plasma was found to be lowest in red-haired mice and *Mitt<sup>mi-wh/mi-wh</sup>* mice but elevated in K14-SCF mice (A), suggesting that melanocyte number and function are positively associated with plasma  $\alpha$ -MSH level. Treatment with a melanocortin agonist, melanotan II (0.5 mg/kg), reduced thermal nociceptive thresholds in red-haired mice (B) ( $n = 10$  per group, except  $n = 9$  for *Mc1r<sup>el/e</sup>* saline), while nociceptive thresholds are increased by the melanocortin antagonist SHU 9119 (1  $\mu$ g/kg) in both black and K14-SCF red-haired mice (C). (D and E) Elevated redheaded nociceptive thresholds are mimicked in *Mc4r* null mice in both mechanical and thermal nociception assays. These elevated thresholds are sensitive to naloxone (F) and naloxonazine (G) but, unlike in red-haired *Mc1r<sup>el/e</sup>* mice (B), cannot be decreased by melanocortin rescue with melanotan II (H). (I) Elevated nociceptive thresholds are not restored by genetic deletion of *Mc4r* in *Mc1r<sup>el/e</sup>* background ( $n = 10, 9, 20,$  and  $6$  per group). Graphs show means  $\pm$  SEM; numbers in parentheses =  $n$  per group.

relative to  $\mu$ -opioid receptors in the central nervous system (CNS), we analyzed publicly available transcriptomic data (“brain atlas”) from six postmortem human brains (30) and identified multiple additional regions showing enrichment for both *MC4R* and *OPRM1* (fig. S6), some of which have been associated with the regulation of pain (31–34). We also investigated the possible correlation between *MC4R* and *OPRM1* across brain regions and patients and found a slight positive correlation (figs. S7 and S8) in the posterior group of nuclei; however, these analyses are limited by the small number of available datapoints. Corroborating these human data, we stained

for both *OPRM1* and *MC4R* proteins in rat brains and found costaining in several regions corresponding to the human brain regions where we observed coexpression of *MC4R* and *OPRM1* mRNAs (fig. S9). It should be noted that *MC4R* antibodies have certain limitations. We tested multiple commercially available antibodies and used an antibody that showed the best signal-to-noise ratio in the arcuate nucleus (fig. S10). These results are consistent with the possibility that melanocortin and opioid signaling may antagonize each other in a cell-autonomous manner. However, it is also possible that other indirect or non-cell-autonomous mechanisms may

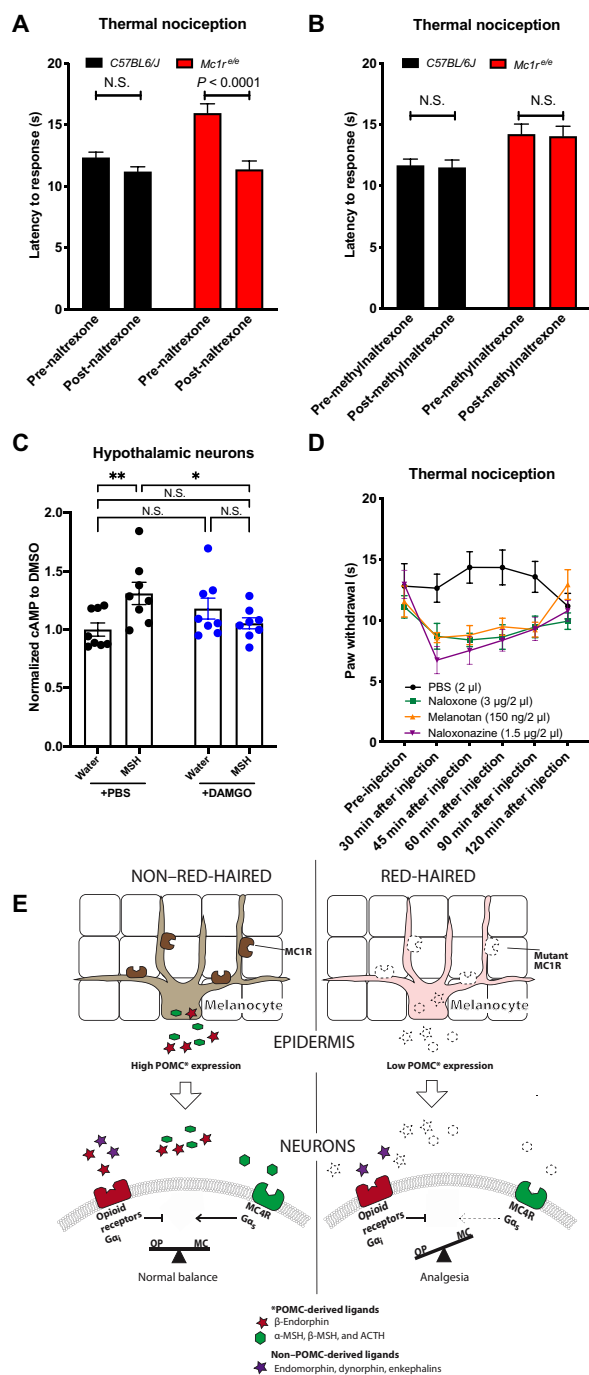


**Fig. 5. Increased central opioid tone regulates basal nociception in red-haired mice.** Blood-brain barrier (BBB)-impermeable methylnaltrexone (10 mg/kg) cannot reverse increased nociception in red *Mc1r<sup>e/e</sup>* mice when injected peripherally (A) ( $n = 20$  for all groups), whereas BBB-permeable naltrexone (10 mg/kg) can (B) ( $n = 20$  per group), suggesting the involvement of CNS regions in the increased nociception. (C) In line with the coexpression of *MC4R* and *OPRM1*, melanocortin and opioid signaling can antagonistically modulate cAMP levels in primary rat hypothalamic neurons. DMSO, dimethyl sulfoxide. (D) Local administration of naloxone, naloxonazine, or melanotan to the periaqueductal gray area (PAG) reduces nociceptive thresholds in red *Mc1r<sup>e/e</sup>* mice ( $n = 9$  using the same mice for all treatments). (E) Summary of the antagonistic opioid-melanocortin model in black and red-haired contexts. Graphs show means  $\pm$  SEM; numbers in parentheses =  $n$  per group.

additionally contribute to increased opioid tone in red-haired *Mc1r<sup>e/e</sup>* mice. For example, heterodimerization of G protein-coupled receptors can affect receptor function (35) and OPRM1 has been previously shown to interact with MC3R (36); therefore, it is possible that formation of different heterodimers might also contribute to the increased opioid tone. However, *Mc1r<sup>e/e</sup>;MC4R<sup>-/-</sup>* mice have similar nociceptive thresholds to *Mc1r<sup>e/e</sup>* mice (Fig. 4I), suggesting that expression of MC4R is not required for maintenance of increased nociceptive thresholds in this background. Therefore, the possible involvement of OPRM1/MC4R heterodimerization is unlikely to be solely responsible for the elevated nociceptive thresholds in the red-haired genetic backgrounds.

The data presented here suggest that elevated nociceptive thresholds found in the red-haired genetic background arise from a reduction in  $\alpha$ -MSH levels caused by decreased POMC production in melanocytes, resulting in diminished MC4R signaling. Lower MC4R signaling, in turn, decreases its antagonism of opioid signaling within the CNS, which, despite diminished  $\beta$ -endorphin production, exhibits no discernible differences in other endogenous opioid ligands in the red hair background. Collectively, this produces a net melanocortin deficiency relative to opioid signaling, which alters the balance in favor of  $\mu$ -opioid receptor-induced analgesia within the red hair background (illustrated in Fig. 5E).

## DISCUSSION

Our observations regarding high nociceptive thresholds in red-haired *Mc1r<sup>e/e</sup>* mice match previous findings of genotype-driven and sex-independent human and mouse nociceptive patterns (4). Also, it should be noted that despite the occasional minor variability in baseline nociceptive measurements (for example, Fig. 4, E and F), we consistently observed a significant difference between black and red-haired mice, suggesting that the differences are much more robust than the minor fluctuations caused by other environmental/technical factors. We provide mechanistic insights for these differential nociceptive thresholds by identifying the role of MC1R variant (red-hair) loss of function in altering the balance of physiologic antagonism between OPRM1 and MC4R through decreased plasma MSH. However, other mechanisms could also contribute to the observed differences. Heterodimerization of OPRM1 with melanocortin receptors (possibly MC3) (36) or additional sex-dependent mechanisms could also contribute to the nociceptive differences observed in melanocortin-deficient mice. Alternatively, melanocortin signaling may directly influence nociception by modifying basal OPRM1 receptor activities such as ion channel activities, G protein coupling, or cAMP inhibition. These possibilities warrant future investigations.

A recent study suggests that only a few polymorphisms in the MC1R coding region predict a differential sensitivity to pain (37). It is possible that although these variants would result in decreased MC1R function (as evidenced by red hair), the loss of function may not impair POMC production in these patients or POMC levels might be somehow compensated through other mechanisms. However, it is challenging to study POMC levels in human populations that can significantly differ in UV shielding due to varying levels of pigmentation and that are exposed to various levels of UV radiation; therefore, the effect of MC1R coding variants on melanocytic POMC expression requires further in-depth examination. It is also possible that in humans, MC1R might regulate POMC in nonmelanocytes as well, which also warrants further studies.

Our study does not distinguish between transcript level–reducing variants and MC1R activity variants, and it is possible that those variants might differentially regulate POMC in mouse and human melanocytes, as hypothesized by Zorina-Lichtenwalter *et al.* (37). However, we have demonstrated that the number of melanocytes also regulates basal nociception, suggesting that besides the loss of MC1R function (as in *Mc1r<sup>el/e</sup>* mice), the absolute number of melanocytes is also an important determinant in nociception. The question of whether the MC1R level altering variations that are associated with differential nociception in humans would also phenocopy the MC1R function loss in mouse models remains to be explored.

POMC induction causes  $\beta$ -endorphin–mediated analgesia after UV exposure (38), whereas in the absence of UV exposure, a reduction in POMC results in melanocortin deficiency–mediated analgesia, as reported here. That both an increase and decrease in POMC can increase analgesia reflects the circumstance wherein a single gene encodes different peptides that activate two opposing pathways. The net effect of POMC depends on the balance of signaling between these two pathways and appears to be affected by differences in basal activities and the presence of other (non–POMC-derived) endogenous ligands. In the red hair background, the decrease in MC4R ligands with low POMC is proportionally large (as MC4R has no known ligands beyond POMC-derived MSH/ACTH) relative to  $\mu$ -opioid receptor ligands where dynorphin, endomorphin, and enkephalin are unchanged (illustrated in Fig. 5E).

While our study focuses on the red hair phenotype, the underlying melanocortin/opioid signaling balance may also account for pain variations among non–red-haired individuals. For example, we observed that *Mc4r* null mice exhibit high nociceptive thresholds like *Mc1r<sup>el/e</sup>* mice, but are not red haired, reflecting an alternative means to alter the melanocortin–opioid balance. Individuals with *MC4R* polymorphisms may also have elevated pain thresholds and altered sensitivities to analgesics similar to those reported in red-haired individuals (4). This study has revealed previously unknown and unexpected insights into the molecular and signaling determinants of basal nociceptive thresholds.

## MATERIALS AND METHODS

### Mice

All experiments were performed with male mice at least 8 weeks of age, with the exception that female mice were used in the experiments of fig. S3. Mice were bred on site. All experiments were performed with approval from the Massachusetts General Hospital Institutional Animal Care and Use Committee. All mice used were on the C57BL/6J background or had been backcrossed to the C57BL/6J background at least 10 generations, except for the *Mc4r<sup>-/-</sup>* strain, which was developed on the 129S background and backcrossed with C57BL/6J for only one generation. However, *Mc4r<sup>-/-</sup>* mice were visually indistinguishable from mice on the C57BL/6J background, making blind experiments possible. *Mc1r<sup>el/e</sup>*, *Tyr<sup>cl/c</sup>*,  $\beta$ -endorphin<sup>-/-</sup>, Dynorphin<sup>-/-</sup>, *Mc4r<sup>-/-</sup>*, and *Oprm1<sup>-/-</sup>* mice were obtained from The Jackson Laboratory (39, 40, 16, 41–43). The K14-SCF strain was a gift from T. Kunisada (44), whereas *Mitf<sup>mi-wh/mi-wh</sup>* mice were a gift from N. Jenkins (45). Mice were used for single experiments, except the same groups of mice were used for measuring thermal and mechanical nociception and for the effects of different pharmacological compounds.

### Drugs

Naloxone hydrochloride (N7758), naltrexone hydrochloride (N3136), and melanotan II acetate salt (M8693) were purchased from Sigma-Aldrich; SHU 9119 (NC9447656), cyprodime hydrochloride (NC9079878), naloxonazine hydrochloride (059110), and DAMGO (11711) were from Thermo Fisher Scientific; and methylnaltrexone bromide (787933) was from McKesson. Morphine was obtained from Patterson Veterinary #078924699. All drug administrations to mice were by intraperitoneal injection.

### Nociceptive testing

The hot plate assay was performed as originally described (46) on a 52°C hot plate with a maximum cutoff time of 20 s, except for the experiments using *Mitf<sup>mi-wh/mi-wh</sup>*, where a cutoff of 30 s was used to enable detecting additive effects of the incorporation of the *Mc1r<sup>el/e</sup>* allele. The von Frey assay was performed as described previously (47). Where possible, the investigator was blinded to the genotypes of the mice.

### PAG cannulation

For cannulation, mice underwent isoflurane anesthesia. Cannulas were positioned to target the ventral lateral PAG (coordinates used bregma –4.5 mm and lateral 0.5 mm) with a custom-made infusion system (P1 Technologies, VA, USA). Custom-made guide cannulas were cut at 2.2-mm length. For intra-PAG injections, an internal cannula of 2.5-mm length was used to administer phosphate-buffered saline (PBS), naloxone, or melanotan under isoflurane anesthesia in 2- $\mu$ l volume. Nociceptive thresholds were then measured using the hot plate assay. The same animals were used to test all pharmacologic agents for this experiment.

### mRNA enrichment analysis

Enrichment analyses of *MC4R* and *OPRM1* in human postmortem brain transcriptomic profiles were performed as described previously (48). Briefly, transcriptomic profiles of six postmortem human brains were downloaded from the Allen Human Brain Atlas (30) in May 2017. To identify brain regions enriched for *OPRM1* and *MC4R*, 190 regions that had transcriptomic profiles from at least four patients were used. We averaged *MC4R* and *OPRM1* expression per region per patient and performed *z* transformation. The obtained *z* values indicate the difference in number of SDs for expression in an individual brain region compared with the average expression across all regions. For *OPRM1* and *MC4R*, we considered a *z* value of  $\geq 1$  to be enriched.

### Epidermal RNA isolation

Black K14-SCF;*Mc1r<sup>E/E</sup>* and red K14-SCF;*Mc1r<sup>el/e</sup>* mice were euthanized by cervical dislocation. Epidermis was isolated from the ears of the animals after dispase digestion for 3 hours at 37°C. Two ears from each mouse were pooled.

### Cell culture

Melan-C cells were grown in Ham's F-10 medium supplemented with 10% fetal bovine serum and 1% penicillin/streptomycin. Cells were serum-starved for various lengths of time before adding 2  $\mu$ M  $\alpha$ -MSH (Phoenix Pharmaceuticals Inc., #043-01), and then RNA was harvested from all samples at the same time 25 hours after initiation of serum starvation. RNA was isolated with RNeasy Mini Kit (74104, Qiagen, NE).



### MC1R knockdown and single clone isolation

Lentivirus was generated in 293T cells. Cells were transfected using 250 ng of vesicular stomatitis virus glycoprotein, 1250 ng of the plasmid PsPAX2, and 1250 ng of luciferase short hairpin RNA (shRNA) (control) or *Mc1r* shRNA. Melan-C cells were plated the day before transduction. After transduction with lentivirus, plates were centrifuged at 3000 rpm for 30 min at 37°C. Transduced cells were selected with 1:1000 puromycin (Thermo Fisher Scientific, catalog no. NC9138068). Single-cell clones were picked up using Scienceware 3.2-mm-diameter cloning discs (Sigma-Aldrich). *Mc1r* shRNA sequences: sh*Mc1r1*, CATC-CCTTCCTGATCTCCATT; sh*Mc1r2*, CGTCACTTTCTTTCTAG-CCAT; sh*Mc1r3*, CCTGATGGTAAGTGTGAGCAT; sh*Mc1r4*, CGTGCTGGAGACTACTATCAT; sh*Mc1r5*, GAGAATGTGCT-GGTTGTGATA.

### Primers and qRT-PCR

For quantitative reverse transcription polymerase chain reactions (qRT-PCRs), the forward and reverse primers for *Pomc* were AA-GAGGCTAGAGGTCATCAG and AGAACGCCATCATCAAGAAC, for OPRM1 CAGGGCTTGTCCTTGTAAGAAA and GACTCGG-TAGGCTGTAAGTGA, for OPRD ATGGCCTCATGCTACTGCG and CACCAGCGTCCAGACGATG, for OPRK TCCCAACTG-GGCAGAATC and GACAGCGGTGATGATAACAGG, for 18S AGGTTCTGGCCAACGGTCTAG and CCCTCTATGGGCTC-GAATTTT, for *Actb* GGCTGTATCCCTCCATCG and CCA-GTTGGTAACAATGCCATGT, and for *Hprt1* TCAGTCAACGGG GGACATAAA and GGGGCTGACTGCTTAACCAG. KAPA SYBR FAST One-Step qRT-PCR (KK4651, Kapa Biosystems) was used for qRT-PCR assays. For quantifying *Pomc* mRNA expression, *Pomc* levels in ear epidermal samples were normalized to the average of 18S, *Actb*, and *Hprt1* to minimize variation.

For measuring levels of opioid receptors in the PAG, micropunches were obtained from freshly isolated PAG tissues. After cervical dislocation, brains were removed in ice-cold PBS. Micropunches (1.5 mm wide) were then obtained, and RNA was isolated as previously described (49).

### cAMP measurements

RPHNs (Lonza, R-HTH-507) were seeded in poly-D-lysine- and laminin-coated wells at a density of 50,000 cells per well. RPHNs were cultured in primary neuron growth medium (Lonza, CC-3256) containing growth supplements (Lonza, CC-4462). Medium was changed every 48 to 96 hours. On day 11 after seeding cells, serum starvation was performed for 30 min, and then cells were treated first with either 1  $\mu$ M DAMGO or PBS for 7.5 min and then with either 1  $\mu$ M [Nle4,D-Phe7]- $\alpha$ -MSH (M8764, Sigma-Aldrich) or water (vehicle control) for 10 min. Cells were incubated at 37°C during treatments. Ten minutes after [Nle4,D-Phe7]- $\alpha$ -MSH or water treatment, cells were lysed and processed for cAMP measurements with cAMP-GLO Assay (V1501, Promega, WI, USA) according to the manufacturer's instructions.

### Radioimmunoassays

Plasma levels of  $\alpha$ -MSH (RK-043-01),  $\beta$ -endorphin (RK-022-06), enkephalin-leucine (RK-024-21), endomorphin-1 (RK-044-10), and dynorphin (RK-021-03) were measured using radioimmunoassay kits (Phoenix Pharmaceuticals Inc., CA, USA) as described previously (38). The specificities of the kits were determined by the manufacturer.

### Histology

All histology experiments were performed in accordance with European Union guidelines (2003/65/CE) and were approved by the Ethical Committee for Animal Research at the Albert Szent-Györgyi Medical and Pharmaceutical Center of the University of Szeged.

### MC4R and OPRM1 double immunohistochemistry

Three male Long-Evans rats (450 to 600 g) were anesthetized with 4 to 5% isoflurane followed by urethane (1.5 g/kg) injection (intraperitoneally) and then transcardially perfused with physiological saline followed by 4% paraformaldehyde and 0.2% picric acid in 0.1 M phosphate buffer (pH 7.2 to 7.3). After removal, brains were post-fixed overnight, embedded in 4% agarose, coronally sectioned at 40- $\mu$ m thickness using a vibrating blade microtome, and harvested in 0.1 M PBS. The following staining procedure was performed at room temperature. All incubations were followed by washing with 0.1 M PBS containing 0.3% Triton X-100 (PBS-X). Sections were incubated successively with 10% normal donkey serum (NDS) in PBS-X for 30 min, a mixture of primary antibodies rabbit anti-MC4R at 1:250 (Alomone Labs, catalog no. AMR-024, RRID:AB\_2039980) and guinea pig anti-OPRM1 at 1:500 (Abcam, catalog no. ab64746, RRID:AB\_1141103) (50) in PBS-X containing 1% NDS (PBS-XD) for 48 hours, and then a mixture of secondary antibodies Alexa Fluor 555-conjugated donkey anti-rabbit immunoglobulin G (IgG) (2  $\mu$ g/ml) (Thermo Fisher Scientific, catalog no. A-31572) and Alexa Fluor 647-conjugated donkey anti-guinea pig IgG (2  $\mu$ g/ml) (EMD Millipore, catalog no. AP193SA6) in PBS-XD for 2 hours. Sections were then counterstained with a fluoro-Nissl solution (Thermo Fisher Scientific, catalog no. N-21479), mounted on gelatin-coated glass slides, and coverslipped with 50% glycerol and 2.5% triethylene diamine in 0.1 M PBS. Corpus callosum, caudate putamen, and arcuate nucleus were analyzed as double and single negative controls.

### Confocal microscopy

Eight-bit images of stained sections were acquired using a Zeiss LSM880 scanning confocal microscope. Low-magnification images of 10- $\mu$ m optical thickness were acquired using a Plan-Apochromat 20 $\times$ /0.8 M27 objective lens (Carl Zeiss) with 2.06- $\mu$ s pixel time and four times frame average at 512  $\times$  512 resolution. High-magnification images of 1.2- $\mu$ m optical thickness were acquired using an alpha Plan-Apochromat 63 $\times$ /1.46 Oil Korr M27 objective lens with 4 $\times$  digital zoom, 4.12- $\mu$ s pixel time, and 16 times frame average at 512  $\times$  512 resolution. Z-stack acquisitions were conducted over 10- to 20- $\mu$ m ranges at 1- $\mu$ m steps, each step of which was at the same setting as it is on the 63 $\times$  objective lens. The power of the lasers was 0.4 to 0.7 mW, which did not induce obvious fading. Acquired raw image files were opened and only linearly processed using a Carl Zeiss software (ZEN Digital Imaging for Light Microscopy, RRID:SCR\_013672), and each image was exported as an eight-bit jpeg file for display.

### Statistics

For pairwise comparisons in the nociceptive assays and serum peptide measurements, two-tailed *t* tests were used. For the cAMP experiment and MSH time course experiment, one-way analysis of variance (ANOVA) was used with Dunnett's multiple comparison test. For *Mc1r* knockdown experiments, one-way ANOVA with Tukey's multiple comparison test was used. For all other experiments, two-way ANOVA with Sidak's multiple comparison test was used. Grubbs test with *P* = 0.05 was used to identify and remove

a single outlier from each of two experiments: in Fig. 1L and in fig. S2B. For all statistical tests, Prism version 7.0a for Mac OS X (GraphPad Software, La Jolla, CA, USA) was used.

## SUPPLEMENTARY MATERIALS

Supplementary material for this article is available at <http://advances.sciencemag.org/cgi/content/full/7/14/eabd1310/DC1>

## REFERENCES AND NOTES

- Y. Xing, J. M. Sonner, E. I. Eger, M. Cascio, D. I. Sessler, Mice with a melanocortin 1 receptor mutation have a slightly greater minimum alveolar concentration than control mice. *Anesthesiology* **101**, 544–546 (2004).
- J. S. Mogil, S. G. Wilson, E. J. Chesler, A. L. Rankin, K. V. S. Nemmani, W. R. Lariviere, M. K. Groce, M. R. Wallace, L. Kaplan, R. Staud, T. J. Ness, T. L. Glover, M. Stankova, A. Mayorov, V. J. Hruby, J. E. Grisel, R. B. Fillingim, The melanocortin-1 receptor gene mediates female-specific mechanisms of analgesia in mice and humans. *Proc. Natl. Acad. Sci. U.S.A.* **100**, 4867–4872 (2003).
- E. B. Liem, C.-M. Lin, M.-I. Suleman, A. G. Doufas, R. G. Gregg, J. M. Veauthier, G. Loyd, D. I. Sessler, Anesthetic requirement is increased in redheads. *Anesthesiology* **101**, 279–283 (2004).
- J. S. Mogil, J. Ritchie, S. B. Smith, K. Strasburg, L. Kaplan, M. R. Wallace, R. R. Romberg, H. Bijl, E. Y. Sartori, R. B. Fillingim, A. Dahan, Melanocortin-1 receptor gene variants affect pain and mu-opioid analgesia in mice and humans. *J. Med. Genet.* **42**, 583–587 (2005).
- E. B. Liem, T. V. Joiner, K. Tsueda, D. I. Sessler, Increased sensitivity to thermal pain and reduced subcutaneous lidocaine efficacy in redheads. *Anesthesiology* **102**, 509–514 (2005).
- T. Andresen, D. Lunden, A. M. Drewes, L. Arendt-Nielsen, Pain sensitivity and experimentally induced sensitisation in red haired females. *Scand. J. Pain* **2**, 3–6 (2011).
- P. Valverde, E. Healy, I. Jackson, J. L. Rees, A. J. Thody, Variants of the melanocyte-stimulating hormone receptor gene are associated with red hair and fair skin in humans. *Nat. Genet.* **11**, 328–330 (1995).
- J. A. D'Orazio, T. Nobuhisa, R. Cui, M. Arya, M. Spry, K. Wakamatsu, V. Igras, T. Kunisada, S. R. Granter, E. K. Nishimura, S. Ito, D. E. Fisher, Topical drug rescue strategy and skin protection based on the role of *Mc1r* in UV-induced tanning. *Nature* **443**, 340–344 (2006).
- D. Mitra, X. Luo, A. Morgan, J. Wang, M. P. Hoang, J. Lo, C. R. Guerrero, J. K. Lennerz, M. C. Mihm, J. A. Wargo, K. C. Robinson, S. P. Devi, J. C. Vanover, J. A. D'Orazio, M. McMahon, M. W. Bosenberg, K. M. Haigis, D. A. Haber, Y. Wang, D. E. Fisher, An ultraviolet-radiation-independent pathway to melanoma carcinogenesis in the red hair/fair skin background. *Nature* **491**, 449–453 (2012).
- A. K. Chakraborty, Y. Funasaka, A. Slominski, G. Ermak, J. Hwang, J. M. Pawelek, M. Ichihashi, Production and release of proopiomelanocortin (POMC) derived peptides by human melanocytes and keratinocytes in culture: Regulation by ultraviolet B. *Biochim. Biophys. Acta* **1313**, 130–138 (1996).
- R. Cui, H. R. Widlund, E. Feige, J. Y. Lin, D. L. Wilensky, V. E. Igras, J. D'Orazio, C. Y. Fung, C. F. Schanbacher, S. R. Granter, D. E. Fisher, Central role of p53 in the suntan response and pathologic hyperpigmentation. *Cell* **128**, 853–864 (2007).
- A. Slominski, J. Wortsman, T. Luger, R. Paus, S. Solomon, Corticotropin releasing hormone and proopiomelanocortin involvement in the cutaneous response to stress. *Physiol. Rev.* **80**, 979–1020 (2000).
- T. Reisine, G. Rougon, J. Barbet, H. U. Afoller, Corticotropin-releasing factor-induced adrenocorticotropin hormone release and synthesis is blocked by incorporation of the inhibitor of cyclic AMP-dependent protein kinase into anterior pituitary tumor cells by liposomes. *Proc. Natl. Acad. Sci. U.S.A.* **82**, 8261–8265 (1985).
- F. René, D. Monnier, C. Gaidon, J. M. Félix, J. P. Loeffler, Pituitary adenylate cyclase-activating polypeptide transduces through cAMP/PKA and PKC pathways and stimulates proopiomelanocortin gene transcription in mouse melanotropes. *Neuroendocrinology* **64**, 2–13 (1996).
- D. C. Bennett, P. J. Cooper, T. J. Dexter, L. M. Devlin, J. Heasman, B. Nester, Cloned mouse melanocyte lines carrying the germline mutations albino and brown: Complementation in culture. *Development* **105**, 379–385 (1989).
- H. W. Matthes, R. Maldonado, F. Simonin, O. Valverde, S. Slowe, I. Kitchen, K. Befort, A. Dierich, M. Le Meur, P. Dollé, E. Tzavara, J. Hanoune, B. P. Roques, B. L. Kieffer, Loss of morphine-induced analgesia, reward effect and withdrawal symptoms in mice lacking the mu-opioid-receptor gene. *Nature* **383**, 819–823 (1996).
- H. Mansikka, C. Zhao, R. N. Sheth, I. Sora, G. Uhl, S. N. Raja, Nerve injury induces a tonic bilateral  $\mu$ -opioid receptor-mediated inhibitory effect on mechanical allodynia in mice. *Anesthesiology* **100**, 912–921 (2004).
- A. L. Vaccarino, R. A. R. Tasker, R. Melzack, Systemic administration of naloxone produces analgesia in BALB/c mice in the formalin pain test. *Neurosci. Lett.* **84**, 103–107 (1988).
- M. M. Lunzer, A. Yekkiral, R. P. Hebbel, P. S. Portoghese, Naloxone acts as a potent analgesic in transgenic mouse models of sickle cell anemia. *Proc. Natl. Acad. Sci. U.S.A.* **104**, 6061–6065 (2007).
- R. W. Clarke, T. W. Ford, The contributions of mu-, delta- and kappa-opioid receptors to the actions of endogenous opioids on spinal reflexes in the rabbit. *Br. J. Pharmacol.* **91**, 579–589 (1987).
- H. Schmidhammer, W. P. Burkard, L. Eggstein-Aeppli, C. F. Smith, Synthesis and biological evaluation of 14-alkoxymorphinans. 2. (–)-N-(cyclopropylmethyl)-4,14-dimethoxymorphinan-6-one, a selective mu opioid receptor antagonist. *J. Med. Chem.* **32**, 418–421 (1989).
- J. I. Székely, E. Migléc, Z. Dunai-Kovács, I. Tarnawa, A. Z. Rónai, L. Gráf, S. Bajusz, Attenuation of morphine tolerance and dependence by alpha-melanocyte stimulating hormone (alpha-MSH). *Life Sci.* **24**, 1931–1938 (1979).
- K. Starowicz, R. Przewlocki, W. H. Gispen, B. Przewlocka, Modulation of melanocortin-induced changes in spinal nociception by mu-opioid receptor agonist and antagonist in neuropathic rats. *Neuroreport* **13**, 2447–2452 (2002).
- K. Tanabe, K. Gamo, S. Aoki, K. Wada, H. Kiyama, Melanocortin receptor 4 is induced in nerve-injured motor and sensory neurons of mouse. *J. Neurochem.* **101**, 1145–1152 (2007).
- V. J. Hruby, D. Lu, S. D. Sharma, A. L. Castrucci, R. A. Kesterson, F. A. al-Obeidi, M. E. Hadley, R. D. Cone, Cyclic lactam alpha-melanotropin analogues of Ac-Nle4-cyclo[Asp5, D-Phe7, Lys10]-alpha-melanocyte-stimulating hormone-(4-10)-NH2 with bulky aromatic amino acids at position 7 show high antagonist potency and selectivity at specific melanocortin receptors. *J. Med. Chem.* **38**, 3454–3461 (1995).
- S. Pierre, T. Eschenhagen, G. Geisslinger, K. Scholich, Capturing adenylyl cyclases as potential drug targets. *Nat. Rev. Drug Discov.* **8**, 321–335 (2009).
- F. René, A. Müller, E. Jover, B. Kieffer, B. Koch, J. P. Loeffler, Melanocortin receptors and  $\delta$ -opioid receptor mediate opposite signalling actions of POMC-derived peptides in CATH.a cells. *Eur. J. Neurosci.* **10**, 1885–1894 (1998).
- M. Chen, Z.-G. He, S.-G. Liu, H.-B. Xiang, Motor cortex-periaqueductal gray-rostral ventromedial medulla neuronal circuitry may involve in modulation of nociception by melanocortinergic-opioidergic signaling. *Int. J. Clin. Exp. Pathol.* **9**, 7897–7907 (2016).
- C. M. Smith, L. L. Walker, T. Leeboonngam, M. J. McKinley, D. A. Denton, A. J. Lawrence, Endogenous central amygdala mu-opioid receptor signaling promotes sodium appetite in mice. *Proc. Natl. Acad. Sci. U.S.A.* **113**, 13893–13898 (2016).
- M. J. Hawrylycz, E. S. Lein, A. L. Guillozet-Bongaarts, E. H. Shen, L. Ng, J. A. Miller, L. N. van de Lagemaat, K. A. Smith, A. Ebbert, Z. L. Riley, C. Abajian, C. F. Beckmann, A. Bernard, D. Bertagnolli, A. F. Boe, P. M. Cartagena, M. M. Chakravarty, M. Chapin, J. Chong, R. A. Dalley, B. D. Daly, C. Dang, S. Datta, N. Dee, T. A. Dolbear, V. Faber, D. Feng, D. R. Fowler, J. Goldy, B. W. Gregor, Z. Haradon, D. R. Haynor, J. G. Hohmann, S. Horvath, R. E. Howard, A. Jeromin, J. M. Jochim, M. Kinnunen, C. Lau, E. T. Lazarz, C. Lee, T. A. Lemon, L. Li, Y. Li, J. A. Morris, C. C. Overly, P. D. Parker, S. E. Parry, M. Reding, J. J. Royall, J. Schulkin, P. A. Sequeira, C. R. Slaughterbeck, S. C. Smith, A. J. Sodt, S. M. Sunkin, B. E. Swanson, M. P. Vawter, D. Williams, P. W. Wornoutka, H. R. Zielke, D. H. Geschwind, P. R. Hof, S. M. Smith, C. Koch, S. G. N. Grant, A. R. Jones, An anatomically comprehensive atlas of the adult human brain transcriptome. *Nature* **489**, 391–399 (2012).
- N. Dafny, W. Q. Dong, C. Prieto-Gomez, C. Reyes-Vazquez, J. Stanford, J. T. Qiao, Lateral hypothalamus: Site involved in pain modulation. *Neuroscience* **70**, 449–460 (1996).
- T. Rizvi, A. Murphy, M. Ennis, M. Behbehani, M. Shipley, Medial preoptic area afferents to periaqueductal gray medulla-output neurons: A combined Fos and tract tracing study. *J. Neurosci.* **16**, 333–344 (1996).
- B. Pan, J. M. Castro-Lopes, A. Coimbra, Central afferent pathways conveying nociceptive input to the hypothalamic paraventricular nucleus as revealed by a combination of retrograde labeling and c-fos activation. *J. Comp. Neurol.* **413**, 129–145 (1999).
- L. Bourgeois, L. Monconduit, L. Villanueva, J.-F. Bernard, Parabrachial internal lateral neurons convey nociceptive messages from the deep laminae of the dorsal horn to the intralaminar thalamus. *J. Neurosci.* **21**, 2159–2165 (2001).
- B. A. Jordan, L. A. Devi, G-protein-coupled receptor heterodimerization modulates receptor function. *Nature* **399**, 697–700 (1999).
- A. Rediger, P. Tarnow, A. Bickenbach, M. Schaefer, H. Krude, A. Grüters, H. Biebermann, Heterodimerization of hypothalamic G-protein-coupled receptors involved in weight regulation. *Obes. Facts* **2**, 80–86 (2009).
- K. Zorina-Lichtenwalter, W. Maixner, L. Diatchenko, Detangling red hair from pain: Phenotype-specific contributions from different genetic variants in melanocortin-1 receptor. *Pain* **161**, 938–948 (2020).
- G. L. Fell, K. C. Robinson, J. Mao, C. J. Woolf, D. E. Fisher, Skin  $\beta$ -endorphin mediates addiction to UV light. *Cell* **157**, 1527–1534 (2014).

39. D. Townsend, C. J. Witkop, J. Mattson, Tyrosinase subcellular distribution and kinetic parameters in wild type and C-locus mutant C57BL/6J mice. *J. Exp. Zool.* **216**, 113–119 (1981).
40. L. S. Robbins, J. H. Nadeau, K. R. Johnson, M. A. Kelly, L. Roselli-Rehffuss, E. Baack, K. G. Mountjoy, R. D. Cone, Pigmentation phenotypes of variant extension locus alleles result from point mutations that alter MSH receptor function. *Cell* **72**, 827–834 (1993).
41. M. Rubinstein, J. S. Mogil, M. Japon, E. C. Chan, R. G. Allen, M. J. Low, Absence of opioid stress-induced analgesia in mice lacking beta-endorphin by site-directed mutagenesis. *Proc. Natl. Acad. Sci. U.S.A.* **93**, 3995–4000 (1996).
42. N. Sharifi, N. Diehl, L. Yaswen, M. B. Brennan, U. Hochgeschwender, Generation of dynorphin knockout mice. *Brain Res. Mol. Brain Res.* **86**, 70–75 (2001).
43. N. Balthasar, L. T. Dalgaard, C. E. Lee, J. Yu, H. Funahashi, T. Williams, M. Ferreira, V. Tang, R. A. McGovern, C. D. Kenny, L. M. Christiansen, E. Edelstein, B. Choi, O. Boss, C. Aschkenasi, C. Zhang, K. Mountjoy, T. Kishi, J. K. Elmquist, B. B. Lowell, Divergence of melanocortin pathways in the control of food intake and energy expenditure. *Cell* **123**, 493–505 (2005).
44. T. Kunisada, S. Z. Lu, H. Yoshida, S. Nishikawa, S. Nishikawa, M. Mizoguchi, S. Hayashi, L. Tyrrell, D. A. Williams, X. Wang, B. J. Longley, Murine cutaneous mastocytosis and epidermal melanocytosis induced by keratinocyte expression of transgenic stem cell factor. *J. Exp. Med.* **187**, 1565–1573 (1998).
45. C. A. Hodgkinson, K. J. Moore, A. Nakayama, E. Steingrimsson, N. G. Copeland, N. A. Jenkins, H. Arnheiter, Mutations at the mouse microphthalmia locus are associated with defects in a gene encoding a novel basic-helix-loop-helix-zipper protein. *Cell* **74**, 395–404 (1993).
46. N. B. Eddy, D. Leimbach, Synthetic analgesics. II. Dithienylbutenyl- and dithienylbutylamines. *J. Pharmacol. Exp. Ther.* **107**, 385–393 (1953).
47. K. Y. Kwan, A. J. Allchorne, M. A. Vollrath, A. P. Christensen, D.-S. Zhang, C. J. Woolf, D. P. Corey, TRPA1 contributes to cold, mechanical, and chemical nociception but is not essential for hair-cell transduction. *Neuron* **50**, 277–289 (2006).
48. O. D. Monte, M. Piva, K. M. Anderson, M. Tringides, A. J. Holmes, S. W. C. Chang, Oxytocin under opioid antagonism leads to supralinear enhancement of social attention. *Proc. Natl. Acad. Sci. U.S.A.* **114**, 5247–5252 (2017).
49. A. M. Kopec, P. D. Rivera, M. J. Lacagnina, R. Hanamsagar, S. D. Bilbo, Optimized solubilization of TRIZOL-precipitated protein permits Western blotting analysis to maximize data available from brain tissue. *J. Neurosci. Methods* **280**, 64–76 (2017).
50. Y. R. Yoon, J.-H. Baik, Melanocortin 4 receptor and dopamine D2 receptor expression in brain areas involved in food intake. *Endocrinol. Metab.* **30**, 576–583 (2015).

**Acknowledgments:** We acknowledge C. Berde, J. Mogil, V. Igras, S. Germana, J. Dellorusso, T. Herbert, A. Wong, M. Kemeny, and C. T. Powell for productive discussions during the early phases of this project and for technical assistance with the experiments and manuscript.

**Funding:** This work was supported by NIH under award number R01AR043369-22 and by grants from the Melanoma Research Alliance, the US-Israel Binational Science Foundation, and the Dr. Miriam and Sheldon G. Adelson Medical Research Foundation (D.E.F. and C.J.W.). L.V.K. was supported by the Rosztoczy Scholarship and the Magyar Állami Eötvös Ösztöndíj provided by the Tempus Közalapítvány. G.K., Y.T., and A.B. were supported by the Momentum program II of the Hungarian Academy of Sciences; EFOP-3.6.1-16-2016-00008 and KKP133871/KKP20 grants of the National Research, Development and Innovation Office, Hungary; 20391-3/2018/FEKUSZTRAT of the Ministry of Human Capacities, Hungary; and EU Horizon 2020 Research and Innovation Program (no. 739593-HCEMM). G.K. was supported by the UNKP-18-3 New National Excellence Program of the Ministry of Human Capacities (UNKP-18-3-503 III-SZTE-16). Y.T. was supported by KAKENHI (18KK0236, 19H03550, and 19H05224). **Author contributions:** Conceptualization: K.C.R., L.V.K., J.M., C.J.W., and D.E.F.; methodology: K.C.R., L.V.K., W.D., S.S., J.M., C.J.W., and D.E.F.; investigation: K.C.R., L.V.K., G.L.F., A.L.H., J.A., W.D., A.Y., J.J.H., M.Y.S., N.T., G.K., Y.T., and A.B.; formal analysis and data curation: K.C.R. and L.V.K.; visualization: K.C.R., L.V.K., G.K., and Y.T.; writing (original draft): K.C.R., L.V.K., and D.E.F.; writing (review and editing): K.C.R., L.V.K., A.B., J.M., C.J.W., and D.E.F.; funding acquisition and supervision: D.E.F. **Competing interests:** A.B. is a shareholder in Amplipex Llc and Neunos Ltd., Hungary, which manufacture biosignal amplifiers and neurostimulator devices. D.E.F. has a financial interest in Soltego Inc., a company developing SIK inhibitors for topical skin darkening treatments that might be used for a broad set of human applications. D.E.F.'s interests were reviewed and are managed by Massachusetts General Hospital and Partners HealthCare in accordance with their conflict of interest policies. The authors declare no other competing interests. **Data and materials availability:** The datasets analyzed during the current study are available in the Allen Brain Atlas Data Portal (<http://human.brain-map.org/static/download>). All other data are available in the main text or the Supplementary Materials. The datasets generated and/or analyzed during the current study are available from the corresponding author upon reasonable request.

Submitted 2 June 2020

Accepted 16 February 2021

Published 2 April 2021

10.1126/sciadv.abd1310

**Citation:** K. C. Robinson, L. V. Kemény, G. L. Fell, A. L. Hermann, J. Allouche, W. Ding, A. Yekkirala, J. J. Hsiao, M. Y. Su, N. Theodosakis, G. Kozak, Y. Takeuchi, S. Shen, A. Berenyi, J. Mao, C. J. Woolf, D. E. Fisher, Reduced MC4R signaling alters nociceptive thresholds associated with red hair. *Sci. Adv.* **7**, eabd1310 (2021).

## Reduced MC4R signaling alters nociceptive thresholds associated with red hair

Kathleen C. Robinson, Lajos V. Kemény, Gillian L. Fell, Andrea L. Hermann, Jennifer Allouche, Weihua Ding, Ajay Yekkirala, Jennifer J. Hsiao, Mack Y. Su, Nicholas Theodosakis, Gabor Kozak, Yuichi Takeuchi, Shiqian Shen, Antal Berenyi, Jianren Mao, Clifford J. Woolf and David E. Fisher

*Sci Adv* 7 (14), eabd1310.  
DOI: 10.1126/sciadv.abd1310

### ARTICLE TOOLS

<http://advances.sciencemag.org/content/7/14/eabd1310>

### SUPPLEMENTARY MATERIALS

<http://advances.sciencemag.org/content/suppl/2021/03/29/7.14.eabd1310.DC1>

### REFERENCES

This article cites 50 articles, 12 of which you can access for free  
<http://advances.sciencemag.org/content/7/14/eabd1310#BIBL>

### PERMISSIONS

<http://www.sciencemag.org/help/reprints-and-permissions>

Use of this article is subject to the [Terms of Service](#)

---

*Science Advances* (ISSN 2375-2548) is published by the American Association for the Advancement of Science, 1200 New York Avenue NW, Washington, DC 20005. The title *Science Advances* is a registered trademark of AAAS.

Copyright © 2021 The Authors, some rights reserved; exclusive licensee American Association for the Advancement of Science. No claim to original U.S. Government Works. Distributed under a Creative Commons Attribution NonCommercial License 4.0 (CC BY-NC).